NeuroImage: Clinical 19 (2018) 147–159

Contents lists available at ScienceDirect

NeuroImage: Clinical

journal homepage: www.elsevier.com/locate/ynicl

# Abnormal functional corticomuscular coupling after stroke

Xiaoling Chen[a], Ping Xie[a,*], Yuanyuan Zhang[a], Yuling Chen[b], Shengcui Cheng[a], Litai Zhang[c]

[a] Yanshan University, Key Lab of Measurement Technology and Instrumentation of Hebei Province, Qinhuangdao, Hebei 066004, China
[b] Institute of Education Science, Tianjin Normal University, Applied Psychology of Tianjin Province, Tianjin 300384, China
[c] Department of Rehabilitation Medicine, The NO.281 Hospital of Chinese People's Liberation Army, Qinhuangdao, Hebei 066100, China

ARTICLE INFO

*Keywords:*
Functional corticomuscular coupling
Flexion synergy
Synkinesis
Separation
Stroke

ABSTRACT

Motor dysfunction is a major consequence after stroke and it is generally believed that the loss of motor ability is caused by the impairments in neural network that controls movement. To explore the abnormal mechanisms how the brain controls shoulder abduction and elbow flexion in "flexion synergy" following stroke, we used the functional corticomuscular coupling (FCMC) between the brain and the muscles as a tool to identify the temporal evolution of corticomuscular interaction between the synkinetic and separate phases. 59-channel electroencephalogram (EEG) over brain scalp and 2-channel electromyogram (EMG) from biceps brachii (BB)/deltoid (DT) were recorded in sixteen stroke patients with motor dysfunction and eight healthy controls during a task of uplifting the arm (stage 1) and maintaining up to the chest (stage 2). As a result, compared to healthy controls, stroke patients had abnormally reduced coherence in EEG-BB combination and increased coherence in EEG-DT combination. Compared to synkinetic stroke patients, separate ones exhibited higher coupling at gamma-band during stage 1 and higher at beta-band during stage 2 in EEG-BB combination, but lower at beta-band during stage 2 in EEG-DT combination. Therefore, we infer that the disorders of efferent control and afferent proprioception in sensorimotor system for stroke patients effect on the oscillation at beta and gamma bands. Patients need integrate more information for shoulder abduction to compensate for the functional loss of elbow flexion in the recovery process, so that partial cortical cortex controlling on the elbow flexion may work on the shoulder abduction during "flexion synergy". Such researches could provide new perspective on the temporal evolution of corticomuscular interaction after stroke and add to our understanding of possible pathomechanisms how the brain abnormally controls shoulder abduction and elbow flexion in "flexion synergy".

## 1. Introduction

Motor dysfunction is a major consequence after stroke (Rathore et al., 2002) and it is generally believed that the loss of motor ability is caused by impairments in neural network that controls movement (Chen et al., 2017). As a typical result, most patients lose their ability to control the independent joint movement (Yao et al., 2009). A major behavior is 'flexion synergy', which means the abnormal coupling between shoulder abduction and elbow flexion in the paretic upper limb (Brunnstrom, 1970; Müller, 1970; Twitchell, 1951). This is also a typically clinical symptom to distinguish the synkinetic and separate phases following stroke. Though several researches point out that stroke patients have increased overlap of shoulder and elbow joint representations at the cortical cortex (Dpt et al., 2005; Miller and Dewald, 2012; Yao et al., 2009), the underlying mechanisms how the cortical overlap synchronous oscillates with the muscles in the flexion synergy remain unknown.

Functional corticomuscular coupling (FCMC) between the motor cortex and the effector muscles, as a neurophysiological measure to synchronization, is considered essential for effective movement control (Grosse et al., 2003). FCMC appears predominantly in the alpha-band (8–14 Hz) during sustained contractions (Raethjen et al., 2002), slow finger movements (Groß et al., 2002; Williams and Baker, 2009) and fast transitions between two force targets (Mehrkanoon et al., 2014), in the beta-band(16–32 Hz) during controlling and maintaining steady-state force output (Baker et al., 1997; Conway et al., 1995; Groß et al., 2000; Halliday et al., 1998; Mehrkanoon et al., 2014; Salenius et al., 1997) and significantly in lower gamma-band range (30–45 Hz) during stronger muscle force production (Brown et al., 1998; Mima and Hallett, 1999) and dynamic force (Mehrkanoon et al., 2014; Omlor et al., 2007). These studies demonstrate that the FCMC in different frequency bands reflects different functional modalities of the sensory and motor systems in healthy people.

Similar studies have been carried out on stroke patients since Mima et al. (2001) first reported that the FCMC for the stroke-affected hand and forearm muscles was reduced compared with that of the unaffected

* Corresponding author.
*E-mail address:* pingx@ysu.edu.cn (P. Xie).

https://doi.org/10.1016/j.nicl.2018.04.004
Received 3 November 2017; Received in revised form 1 February 2018; Accepted 1 April 2018
Available online 04 April 2018

side during weak tonic contraction tasks. Fang et al. (2009), Meng et al. (2009), and von Carlowitz-Ghori et al. (2014) also reported that stroke patients had significantly lower FCMC on the stroke-affected side. The decrease in FCMC indicates that the impairments in the lesioned hemisphere may lead to discontinuity of information transmission in the sensory-motor system. However, Braun et al. (2007) observed that maximal FCMC in some patients with excellent recovery was higher than that in healthy controls, and Graziadio et al. (2012) reported that there were no FCMC differences between stroke patients and healthy controls. Rossiter et al. (2013) revealed that the peak of corticomuscular coherence in both beta and gamma bands were more widespread in stroke patients, including both the contralateral sensorimotor cortex and the contralesional hemisphere during a simple isometric grip. Although the above studies do not provide uniform conclusions on functional coupling and temporal coordination, they indicate that the FCMC between the motor cortex and the muscles can be considered an assessment mechanism for motor recovery.

In the literatures, the above features of the FCMC have been identified during a simple task in healthy individuals, i.e. hand grip or finger press with steady-state force (Baker et al., 1997; Conway et al., 1995; Groß et al., 2000; Halliday et al., 1998; Mehrkanoon et al., 2014; Salenius et al., 1997) or dynamic force (Mehrkanoon et al., 2014; Omlor et al., 2007). However, it is hard for stroke patients with flexion synergy to completely perform the fine and complicated movements with their affected hands. What is more, above these tasks having no connection with shoulder abduction or elbow flexion are meaningless in the research of the flexion synergy. Within a mass of clinical assessment systems, many movements referring to shoulder abduction and elbow flexion, such as 'uplift the affected hand to reach the ipsilateral ear', 'turn the hand behind to reach the midline of the spine' and so on, are used to check the functional rehabilitation state for upper limb. In Shang Tianmin (STM) test system, the movement of 'uplift the affected hand to reach the ipsilateral ear' are often used to distinguish the synkinetic and separate phases for stroke, because the accomplishment of this movement mainly depends on large scale of elbow flexion and little scale of shoulder abduction. However, the scale of elbow flexion and shoulder abduction is often changed for stroke patients, especially for stroke patients with synkinesis (Dpt et al., 2005; Miller and Dewald, 2012; Yao et al., 2009). In this study, we try to explore these changes from the view of synchronous oscillation between the brain and the muscles. Before embarking on this research, we hypothesize that the oscillatory activity between the motor cortex and the effector muscles may be decreased for stroke patients but gradually increased in the recovery process.

Above all, we used the FCMC as a tool to identify the temporal evolution of corticomuscular interaction between the synkinetic and separate phases. We explore the abnormal mechanisms how the brain controls shoulder abduction and elbow flexion in "flexion synergy" after stroke. To investigate this, we used the coherence method to analyze the electroencephalogram (EEG) and electromyogram (EMG) data synchronously recorded during the task of uplifting their arms and maintaining up to the chest. Such researches could provide new perspective on the temporal evolution of corticomuscular interaction after stroke and add to our understanding of possible pathomechanisms how the brain to abnormally control shoulder abduction and elbow flexion in "flexion synergy".

## 2. Materials and methods

### 2.1. Subjects

Sixteen stroke patients who had persistent dys-coordination of the right upper limb (Table 1; mean age, 50.50 ± 15.41 years; range, 28–72 years; 9 male) and eight healthy controls (mean age, 60.5 ± 6.26 years; range, 52–70 years; 4 male) without any history of neurological disease were enrolled in this study. All patients were first-time stroke victims and their lesion sites are marked in Table 1. According to the STM test for assessing the upper limb, all patients were divided into synkinetic and separate phases. All subjects were tested according to the Oldfield questionnaire (Oldfield, 1971). The experiment was in accordance with the declaration of Helsinki and gained consent and approval of the ethical review board of Yanshan University. All participants have given informed consent. They had no experience with similar experiments.

### 2.2. Data recording and experimental paradigm

#### 2.2.1. Experiment paradigm

During the experimental session, the subjects sat in an electrically shielded and dimly lit room. All subjects need to perform the task of uplifting the arm to measure the "flexion synergy" as shown in the Fig. 1. Visual feedback was provided for the subjects via a monitor with video and tune. Before experiment, all subjects were instructed to place their affected hands to the contralateral waist as the Fig. 1(A) was shown. At the 2th sec after recording the data, the subjects need to slowly lift their hands up to the chest within 3 s according to the tip with speed at 15°/s (stage 1). Subsequently, the motion up to the chest need maintain for 3 s (stage 2). The task included 20 sessions with 60s breaks between each session to avoid fatigue. Fig. 1(B) showed one subject performed the task.

#### 2.2.2. Motion, EEG and EMG data recording

EEG and EMG data were recorded synchronously by 64 channels NeuroScan system (Synamp2, Compumedics Inc., Charlotte, NC, USA), and the motion data was also synchronously by the Perception legacy system (TM-SI-8-STD, NoitomTechnology Ltd., Beijing, China). EEG signals were recorded from 59 scalp positions using the international 10–20 system referenced to ears mastoid (Fig. 1(C)). EMG signals were recorded from the deltoid (DT) and biceps brachii (BB) (Fig. 1(D)). Before the electrode application, the hair needed to clean, and the skin surface was cleaned with alcohol. The EEG and EMG were amplified (1000), band-pass filtered (0.5–150 Hz) and digitized (1000 Hz).

### 2.3. Data processing and analysis

#### 2.3.1. Data preprocessing

Data analysis was conducted offline in Matlab environment. First, the motion data with large amplitude artifacts were excluded. The corresponding EMG and EEG signals of those sections were discarded, too. To avoid the influence of the number of segments on coherence, the bootstrapping was performed to select the same number of segments for subsequent analysis. After visual inspection, we designed a combined filter to remove these artifacts in raw EEG recordings, such as EMG, Electrooculogram (EOG), electrocardiograph (ECG) and power signal of 50 Hz. First, mean and standard deviation rejected outlier points. Then, an adaptive notch filter (Stoica and Nehorai, 1988) was used to remove the 50 Hz power signal, and a high-pass filter was used to remove baseline drift. After that, Informax-based independent component analysis (ICA) was used to remove the ECG and EOG signals. Finally, canonical correlation analysis (CCA) was implemented to remove the EMG signal from the EEG signal (De Clercq et al., 2006). Compared to EEG signals, the interferences in EMG signals were easily removed. The main interference sources in EMG were also the 50 Hz power signal, electromagnetic radiation and the internal electronic noise interference of instruments. According to these problems, an adaptive notch filter was used to remove the 50 Hz power signal, and a 0.5–150 Hz bandpass filter was used to remove the direct current high frequency interference. To enhance the motor neuron firing rate (Myers et al., 2003; Yao et al., 2007), EMG signals were rectified before subsequent analysis, although previous research (McClelland et al., 2012) suggests rectification having influence on EMG signals. However, our result showed that coherence between EEG and rectified EMG is more obvious than that between EEG and non-rectified EMG.

**Table 1**
Demographic information of stroke patients.[a]

| Patients | Age | Months since stroke | Gender | STM test[b] | | Lesion site | Stroke type |
|---|---|---|---|---|---|---|---|
| | | | | Affected | Unaffected | | |
| 1 | 44 | 5 | M | 7 | 11 | R Periventricular | Ischemia |
| 2 | 52 | 3 | F | 3 | 7 | R Temporal Lobe, External Capsule | Ischemia |
| 3 | 37 | 6 | M | 6 | 11 | L Frontal Lobe, Centrum Semiovale, Periventricular | Ischemia |
| 4 | 55 | 2 | M | 6 | 10 | Pons | Ischemia |
| 5 | 47 | 12 | M | 4 | 9 | R Basal Ganglia | Hemorrhage |
| 6 | 66 | 8 | M | 4 | 10 | Pons | Ischemia |
| 7 | 59 | 3 | F | 3 | 8 | R Basal Ganglia | Ischemia |
| 8 | 66 | 14 | F | 4 | 8 | L Basal Ganglia | Ischemia |
| 9 | 76 | 19 | F | 6 | 9 | L Basal Ganglia, Inferior temporal lobe | Hemorrhage |
| 10 | 72 | 6 | M | 3 | 9 | R Inferior MCA territory | Ischemia |
| 11 | 28 | 23 | M | 7 | 11 | L Corona radiata | Ischemia |
| 12 | 62 | 6 | F | 5 | 10 | R Inferior MCA territory | Hemorrhage |
| 13 | 28 | 18 | F | 3 | 9 | R Anterior choroidal artery territory | Hemorrhage |
| 14 | 45 | 14 | M | 4 | 9 | L Basal Ganglia | Ischemia |
| 15 | 38 | 12 | M | 5 | 8 | R External Capsule | Ischemia |
| 16 | 33 | 7 | F | 6 | 10 | R Basal Ganglia | Hemorrhage |

[a] F, female; M, male; R, right brain; L, left brain.
[b] In the STM test, the recovery for upper limb was evaluated by a score ranging from 1 to 12. The better recovery, the higher score. If the score is less than or equal to 4, it means that the patient is at the synkinetic phase; if the score is > 4, it means that the patient steps into the separate phase.

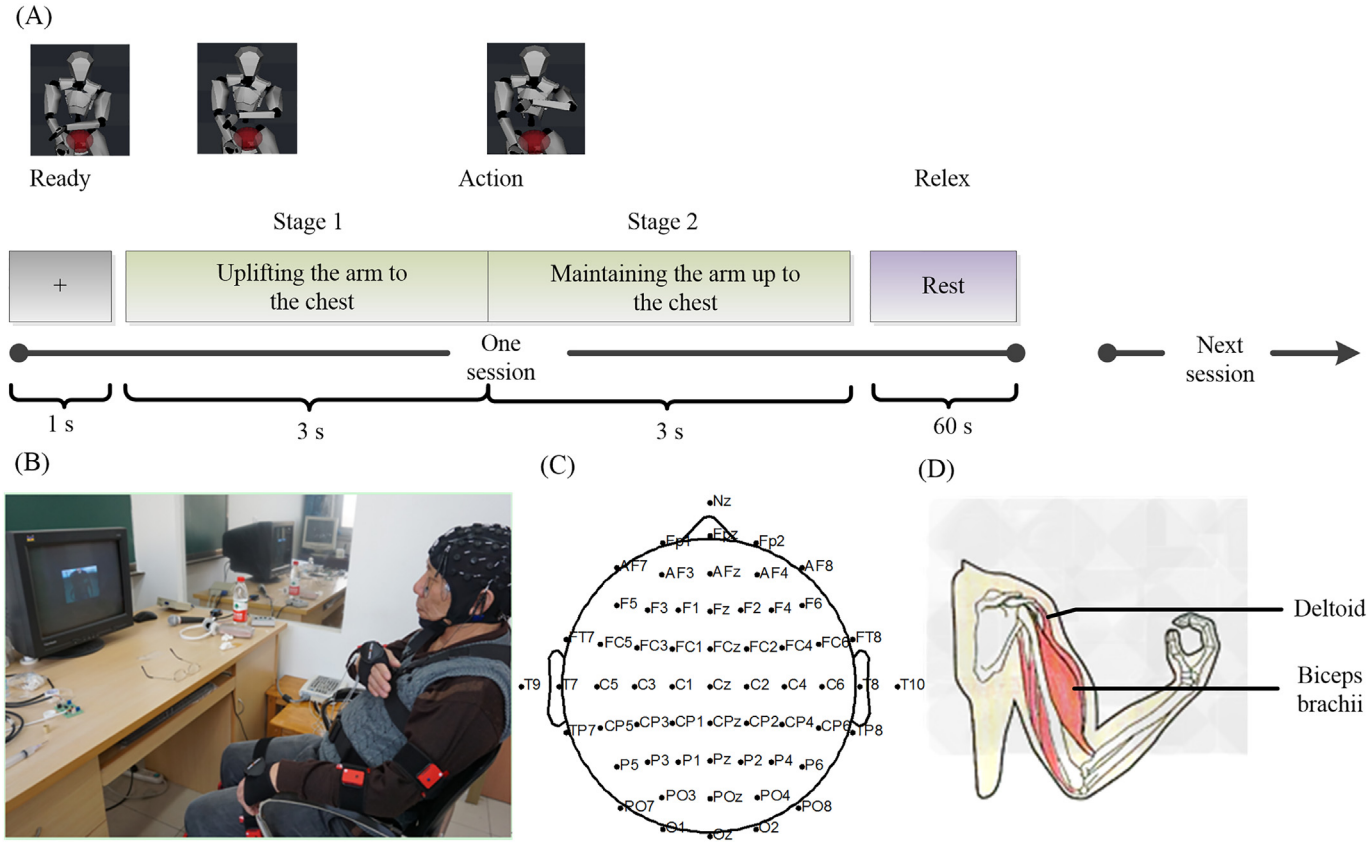


**Fig. 1.** Experiment setup. Subjects were instructed to place their affected hands to the contralateral waist. At the 2th sec after recording the data, the subjects need to slowly lift their hands up to the chest within 3 s according to the tip with speed at 15°/s (stage 1). Subsequently, the motion up to the chest need to maintain for 3 s (stage 2). (A) The flow of the experimental task. (B) One subject performed the task. (C) 59-channel scalp positions. (D) 2-channel EMG positions for the deltoid (DT) and biceps brachii (BB) muscles.

### 2.3.2. Coherence and time-frequency coherence

To measure the correlation between EEG and EMG signals, coherence (Mima and Hallett, 1999) was calculated with a fast Fourier transform algorithm. Let $X$ and $Y$ denote the EEG and EMG signals, respectively. Coherence value, $Coh_{X,Y}(f)$, was calculated on the basis of the following formulate according to the following equation

$$Coh_{X,Y}(f) = \frac{|P_{XY}(f)|^2}{P_{XX}(f)P_{YY}(f)} \quad (1)$$

where $P_{XX}(f) = \frac{1}{N}\sum_{j=1}^{N} X_j(f)X_j^*(f)$ and $P_{YY}(f) = \frac{1}{N}\sum_{j=1}^{N} Y_j(f)Y_j^*(f)$ are the power spectra for $X$ and $Y$ at the same frequency, respectively. $P_{XY}(f) = \frac{1}{N}\sum_{j=1}^{N} X_j(f)Y_j^*(f)$ is the cross-spectrum for the EEG signal in

channel $X$ and the EMG signal in channel $Y$ at a given frequency $f$. Coherence values, $Coh_{X,\ Y}(f)$, is between 0 and 1.

To further capture the changes in FCMC during the execution of the whole task, time-frequency coherence (Grinsted et al., 2004) was used. The time-frequency representation $X(t,f)$ and $Y(t,f)$ were computed as:

$$X(t,f) = \int_{-\infty}^{+\infty} x(t+\tau)w(\tau,f)d\tau,\ Y(t,f) = \int_{-\infty}^{+\infty} y(t+\tau)w(\tau,f)d\tau \tag{2}$$

where $t$ is time relative to the onset of a trial; $x(t)$ and $y(t)$ are the original EEG and EMG signals, respectively; $w(t,f)$ is given by $w(t,f) = \exp(2\pi ft i - t^2/2\sigma^2)$, $i = \sqrt{-1}$. The coherence $Coh_{X,\ Y}(t,f)$ was calculated as

$$Coh_{X,Y}(t,f) = \frac{|P_{XY}(t,f)|^2}{P_{XX}(t,f)P_{YY}(t,f)} \tag{3}$$

where $P_{XX}(t,f)$ and $P_{YY}(t,f)$ are the power of $X$ and $Y$ as a function in time-frequency domain.

#### 2.3.3. Calculation of significant level

Coherence was considered significant ($P < 0.05$) if it exceeded $C_{0.05}$ given by

$$CL = 1 - 0.05^{1/(N-1)} \tag{4}$$

This formula was given by Rosenberg et al. (1989) for Fourier transform based coherence calculations.

### 2.4. Statistical analysis

To quantitatively analyze the significant coherence between the EEG and EMG signals in a specific band ($f_l$~$f_h$) and avoid the differences from the bandwidth, the normalized significant area, defined as $A_{coh(f_l\sim f_h)}$, was calculated as

$$A_{coh(f_l\sim f_h)} = \frac{1}{f_h - f_l}\sum_{f_l\sim f_h}\Delta f\cdot(Coh_{X,Y}(f) - CL) \tag{5}$$

where $\Delta f$ denotes frequency resolution; We defined $A_{coh}$ as the normalized significant area over whole frequency bands (< 60 Hz). After that, repeated measures analysis of variance (rANOVA) was performed to investigate the differences between stroke patients and healthy controls in both stage 1 and stage 2.

Similarly, to further exam whether the $A_{coh(f_l\sim f_h)}$ values were contributed by potential EEG or EMG spectral power differences in specific band ($f_l$~$f_h$), we first calculated the normalized area under the SP curve, $A_{pow(f_l\sim f_h)}$, by

$$A_{pow(f_l\sim f_h)} = \frac{1}{f_h - f_l}\sum_{f_l\sim f_h}\Delta f\cdot SP_X(f) \tag{6}$$

where $SP_X(f) = \frac{1}{n}\sum_{i=1}^{n} X_i(f)X_i^*(f)$ means the spectral power for a given channel $X_i(f)$ represents the Fourier transform of the $X$ for a given segment number ($i = 1, 2, \cdots, n$) and '*' indicates the complex conjugate). After that, person correlation was applied to analyze the relationship between the $A_{coh(f_l\sim f_h)}$ and $A_{pow(f_l\sim f_h)}$ values.

Additionally, in our study, the mean values of the angular acceleration during stage 1 and the angle during stage 2 were calculated for each subject. For each subject, the error $AA\_MSE_j$ was calculated between the actual angular acceleration ($AA_j^i$) at each time point and the mean value ($\bar{AA}_j$) across all time points throughout the range from 2 to 5 s for stage 1. The error $AA\_MSE_j$ between $AA_j^i$ and $\bar{AA}_j$ in the $j$th epoch was calculated as

$$AAMSE_j = \frac{1}{N}\sum_{i=1}^{N}(AA_j^i - \bar{AA}_j) \tag{7}$$

where $i$ is the sampled point in one epoch, $j$ is the $j$th epoch, and $N$ is the number of time point throughout the range from 5 to 8 s. For each subject, the mean error $AA\_MSE_{mean}$ over all epochs were calculated as following

$$AAMSE_{mean} = \frac{1}{M}\sum_{j=1}^{M} AAMSE_j \tag{8}$$

where $M$ represents the number of epoch for each subject.

The error $A\_MSE_j$ was calculated between the actual angle ($A_j^i$) at each time point and the mean value ($\bar{A}_j$) across all time points throughout the time range from 5 to 8 s for stage 2. For each subject, the mean error $A\_MSE_{mean}$ over all epochs can be also obtained following the similar formula (Eq. (8)). To investigate possible influence of the motor performance on the CMC in two stages, we divided the $AA\_MSE_{mean}$ values into two groups. The first group, hereafter named "good", contained the lower $AA\_MSE_{mean}$ values, and the second named "bad" with higher ones. The former group possessed lowest errors while the latter one was at the opposite extreme. We calculated the $A_{coh}$ value for all patients, and then analyzed the $A_{coh}$ distribution among the two groups. These were suitable to stage 2. In this study, an alpha of $P < 0.05$ was considered significant. SPSS 19.0 for windows (SPSS Inc., Chicago, IL, USA) was used for all statistical computations.

The whole procedure for angle, angular acceleration, EEG and EMG signals was shown in Fig. 2.

## 3. Results

### 3.1. Motor performance

The performed task in STM test has a reference range for the elbow and shoulder joint movement. In general, the flexion for elbow joint as the main action is within large range (50° to 100°), while the abduction for shoulder joint as the complementary action is within small range (−10° to 10°). Considering that the flexion synkinesis for upper limb mainly refers to the coupling between elbow flexion and shoulder abduction, the shoulder flexion was excluded in this study. To describe the change of angle signals (elbow and shoulder joint) during stage 1 and stage 2, the trajectory of angle signals of elbow flexion and shoulder abduction were showed in Fig. 3(A), (B) and (C).

As Fig. 3(A), (B) and (C) were shown, there were 55.38°–101.67° flexion for elbow and −9.62°–9.34° abduction for shoulder in controls, which was almost matched the standard conditions. However, there were 60.87°–88.21° flexion for elbow and −5.29°–46.26° abduction for shoulder in synkinesis, and 56.69°–95.83° flexion for elbow and −8.44°–26.37° abduction for shoulder in separation. It was obvious that stroke patients expended the abduction range for shoulder joint. During the stage 1 from 2 s to 5 s, the angle signals showed approximately linearly increased. As we calculated, the angular accelerations were 7.51 ± 1.73, 10.88 ± 1.58, 14.33 ± 1.72 for elbow joint and 14.25 ± 1.59, 8.89 ± 0.75, 5.11 ± 0.80 for shoulder joint in synkinesis, separation and control, respectively. During the stage 2 from 5 s to 8 s, the angle signal held a relative stability. The angles were 81.38 ± 4.88, 89.58 ± 5.00, 98.37 ± 2.29 flexion for elbow joint and 41.63° ± 3.18°, 22.15° ± 4.06°, 8.34° ± 0.87° abduction for shoulder joint in synkinesis, separation and control, respectively.

Fig. 3(D), (E), (F) and (G) showed box-plots of the angular acceleration and angle signals in elbow and shoulder joints for synkinetic patients, separate patients and healthy controls, respectively. One-way analysis of variance (ANOVA) was used to analyze the angular acceleration or angle differences among synkinesis, separation and control. After that, we performed pairwise comparison with Bonferroni correction. Significant differences existed between each pair for synkinetic patients, separate patients and healthy controls. Compared to healthy controls, stroke patients, especially for synkinesis, exhibited poor ability for maintaining the movement trajectory. Larger scale of shoulder abduction was in synkinetic patients compared to separate

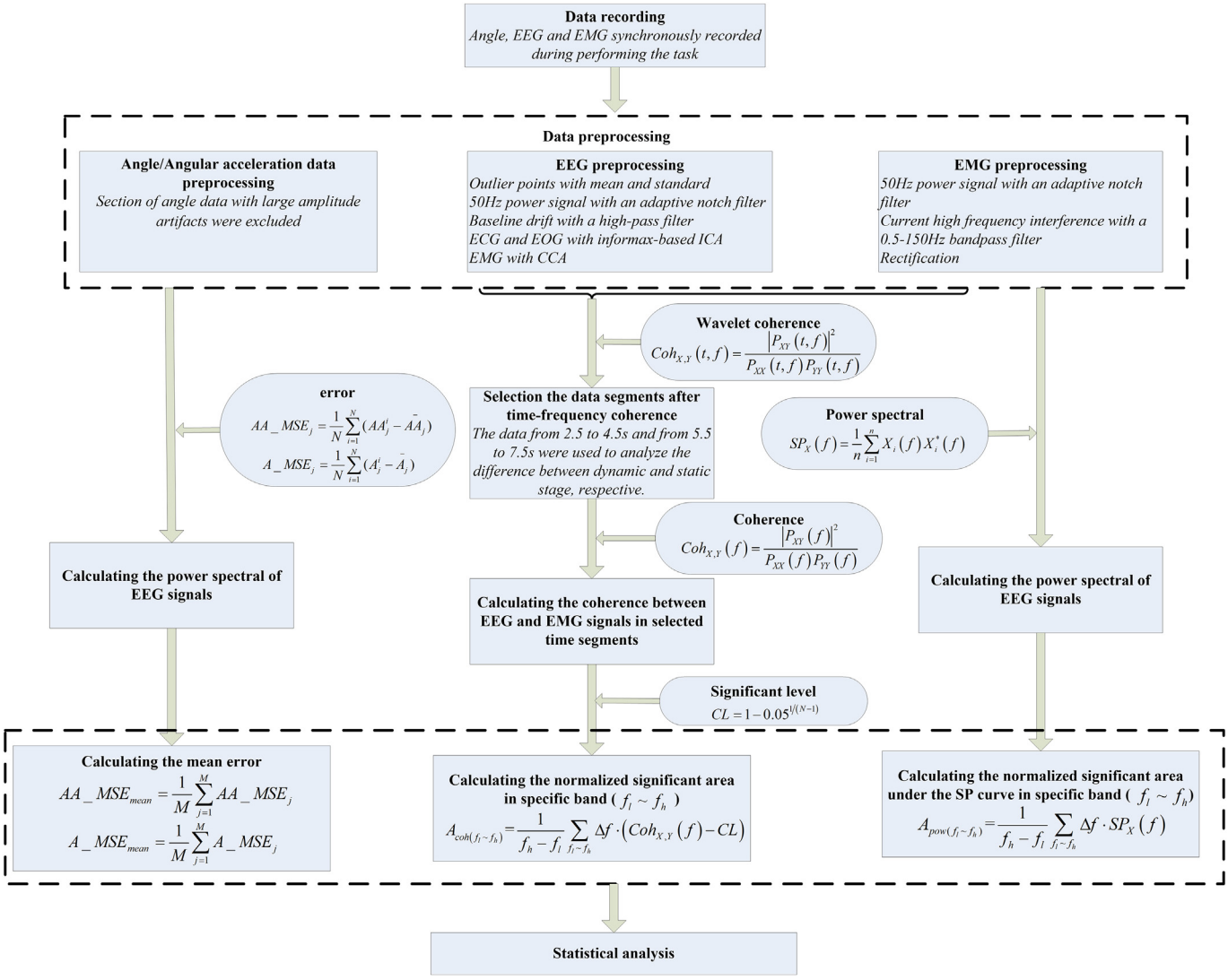


**Fig. 2.** Schematic diagram.

patients and healthy controls. All these indicated that the task performed for stroke patients need shoulder abduction to compensate for the insufficient of flexion with elbow joint.

### 3.2. EEG/EMG power spectral

Considering large differences of the joint angle among the synkinetic patients, separate patients and healthy controls, we further explored the differences of the EMG signal in BB and DT muscles. Fig. 4 showed that the trajectory of EMG signals of BB and DT muscles in time domain (the first and second line), and the power spectral in time-frequency domain (the third and fourth line) for synkinesis, separation and control, respectively. As shown in this figure, both amplitude and power spectral for BB and DT muscles were different among the synkinetic patients, separate patients and healthy controls. For healthy controls in standard posture, the BB muscle as agonistic muscle was contracted largely and the EMG signal of BB was stronger, but the DT muscle as agonistic muscle was contracted smaller and the EMG signal of DT muscle was weaker. However, in fact, for affected side with synkinesis or separation, the EMG signal of BB muscle was lower, but the EMG signal of DT muscle was larger than that in controls. And further analysis showed that the EMG signal of BB muscle was also lower and the EMG signal of DT muscle was larger for patients with synkinesis than that for those with separation. All these indicated plenty of motor neurons in DT muscle were activated to trigger large scale of shoulder abduction, which was consistent with the change of the angle signals in stroke patients.

### 3.3. Corticomuscular coherence

Fig. 5 showed the topographic distribution of the $A_{coh}$ values in both EEG-BB and EEG-DT combinations for the synkinesis, separation and control, respectively. Though stroke patients had lower coupling in EEG-BB combination and higher coupling in EEG-DT combination, the strongest interaction was localized in the left motor cortex (CP3, CP5, FC3, FC5, C3) contralateral to the right hand. In the subsequent analysis the coherence was analyzed based on the mean values of EEG signals over CP3, CP5, FC3, FC5, C3 and C5 channels.

In order to further describe the change of the FCMC during stage 1 and 2, Fig. 6 showed average EEG-EMG coherence across all subjects, which indicated a significant difference between the stroke patients and control subjects at beta and gamma bands in EEG-BB and EEG-DT combinations. Fig. 6(A) and (B) showed its coherence with the scalp areas for the synkinetic patients, (C) and (D) for separate patients, and (E) and (F) for healthy controls. Overall, the FCMC in EEG-BB combination was larger than that in EEG-DT combination. Additionally, the FCMC mainly focused on high frequency-band under stage 1, while low frequency-band under stage 2. To further analyze the specific band on

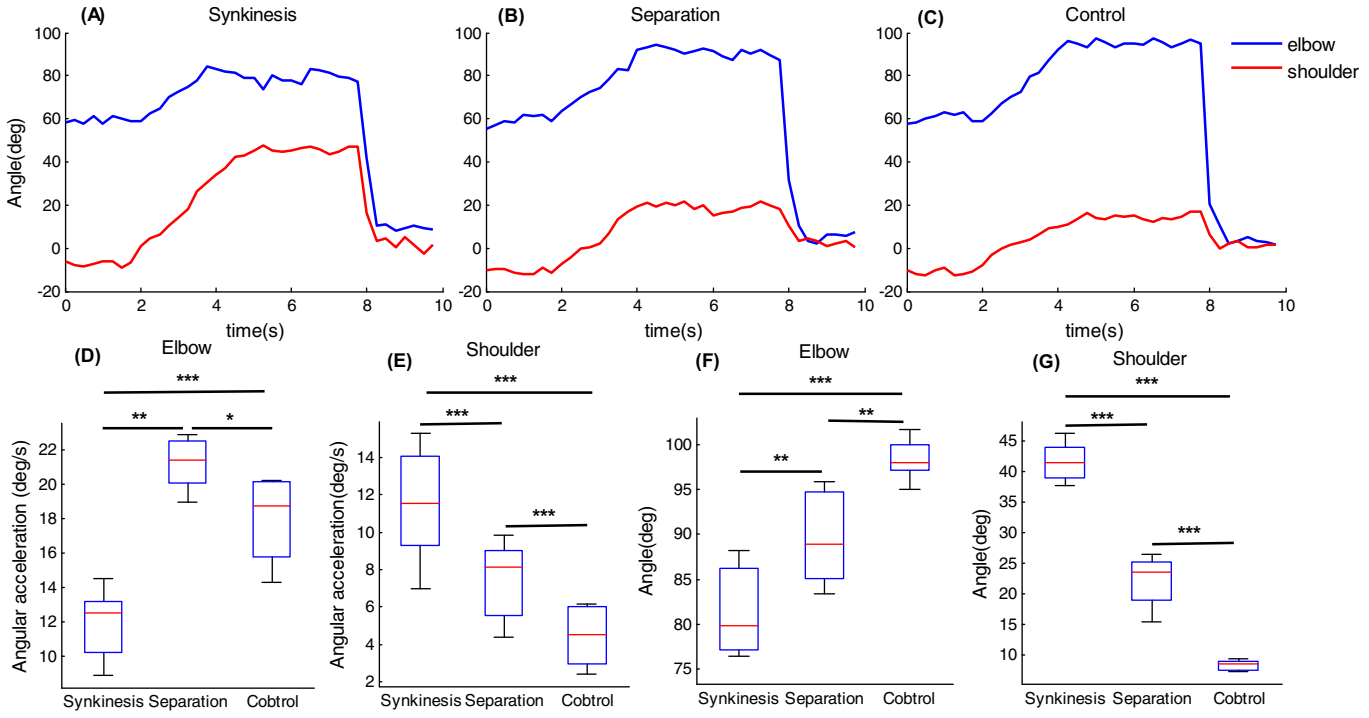


**Fig. 3.** The trajectory of angle signals and box-plots of angular acceleration and angle signals in elbow and shoulder joints for synkinesis, separation and control, respectively. (A), (B) and (C) showed the trajectory of angles in elbow and shoulder joints for synkinesis, separation and control, respectively. (D), (E) showed the box-plot of angular acceleration in elbow and shoulder during stage 1 and (F), (G) showed for angle during stage 2 for synkinesis, separation and control, respectively. The asterisk in the box denoted the significance, *p < 0.05, **p < 0.01, ***p < 0.001.

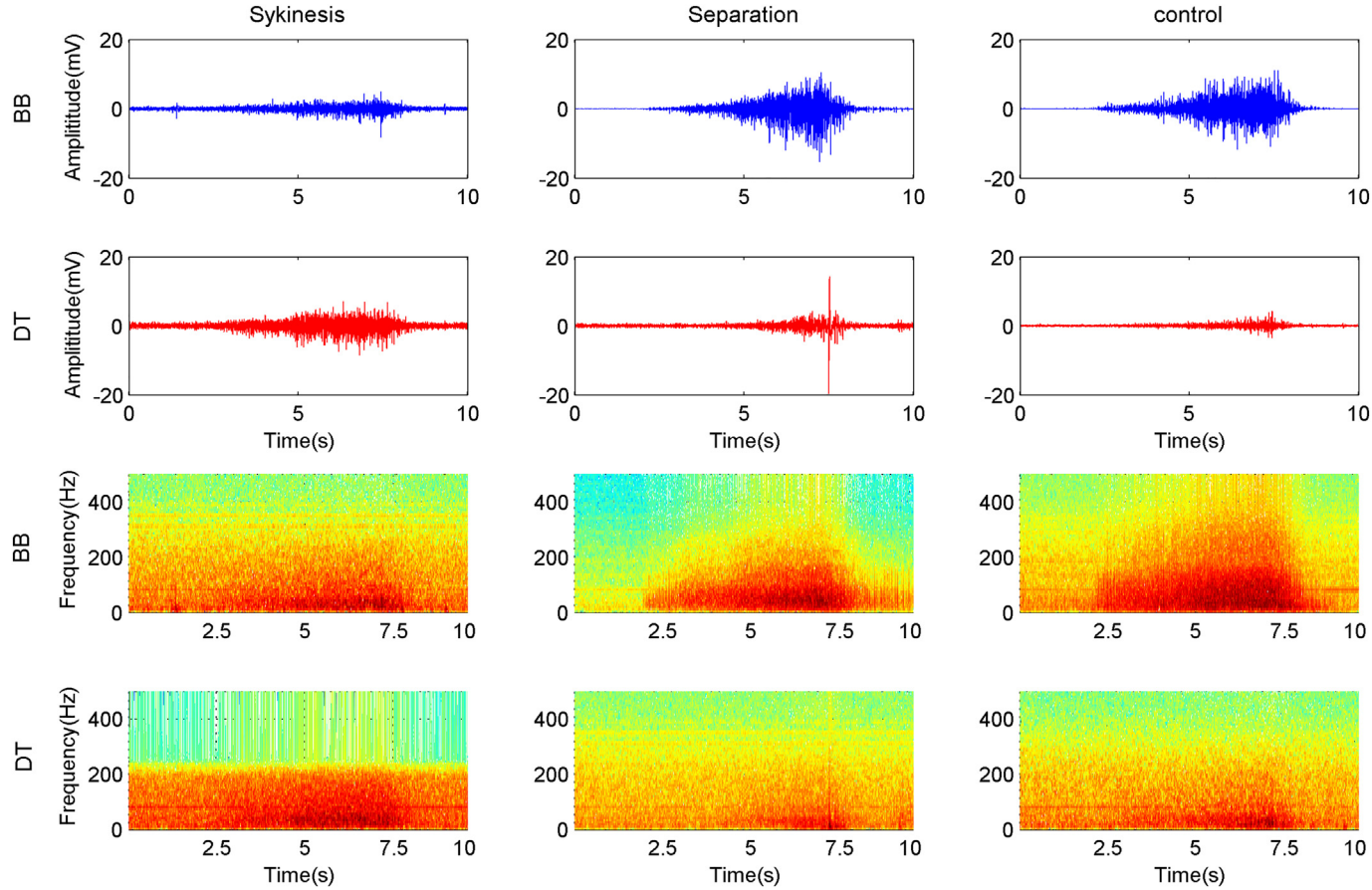


**Fig. 4.** The trajectory of EMG signals in both BB and DT muscles in time domain and the power spectral of EMG signals in both BB and DT muscles in time-frequency domain for synkinesis, separation and control, respectively.

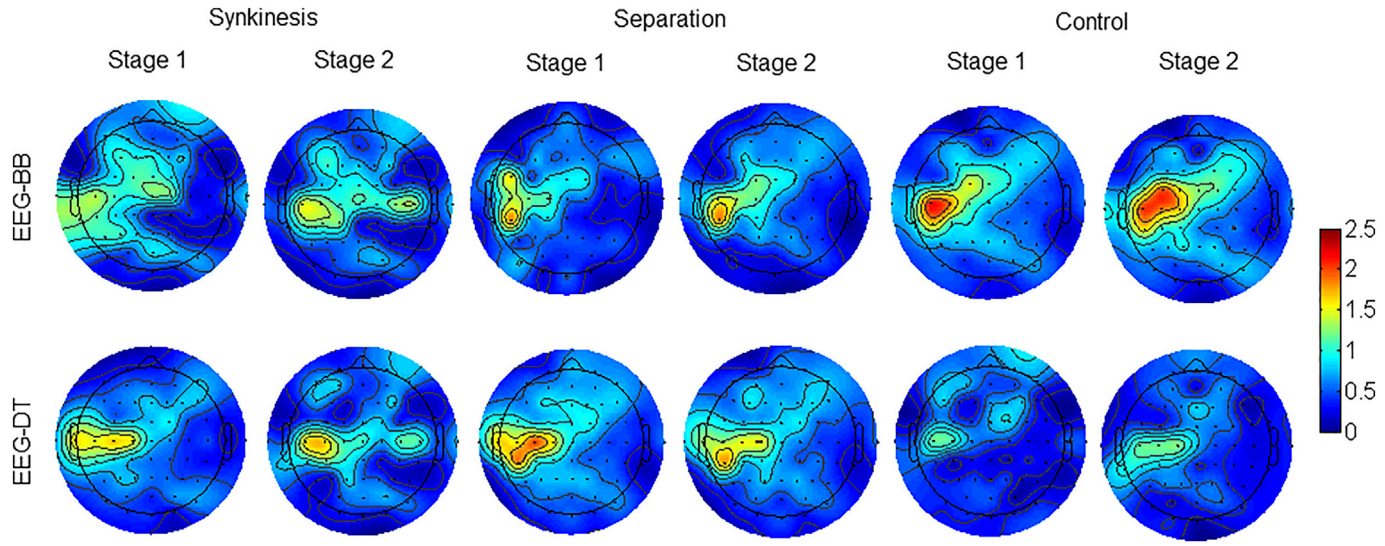


**Fig. 5.** Topographic distribution of the $A_{coh}$ values in both EEG-BB and EEG-DT combinations for synkinesis, separation and control, respectively.

which the FCMC focused, we selected the time range where the FCMC distributed steadily to calculate coherence.

Fig. 6(G), (H), (I) and (J) showed the coherence spectra for healthy controls and stroke patients calculated throughout the time range from 2.5 to 4.5 s and from 5.5 to 7.5 s for stage 1 and stage 2, respectively. For healthy controls, subjects exhibited significant coherence corresponding primarily to the gamma and beta bands in EEG-BB combination for stage 1 and stage 2, respectively, and almost absent

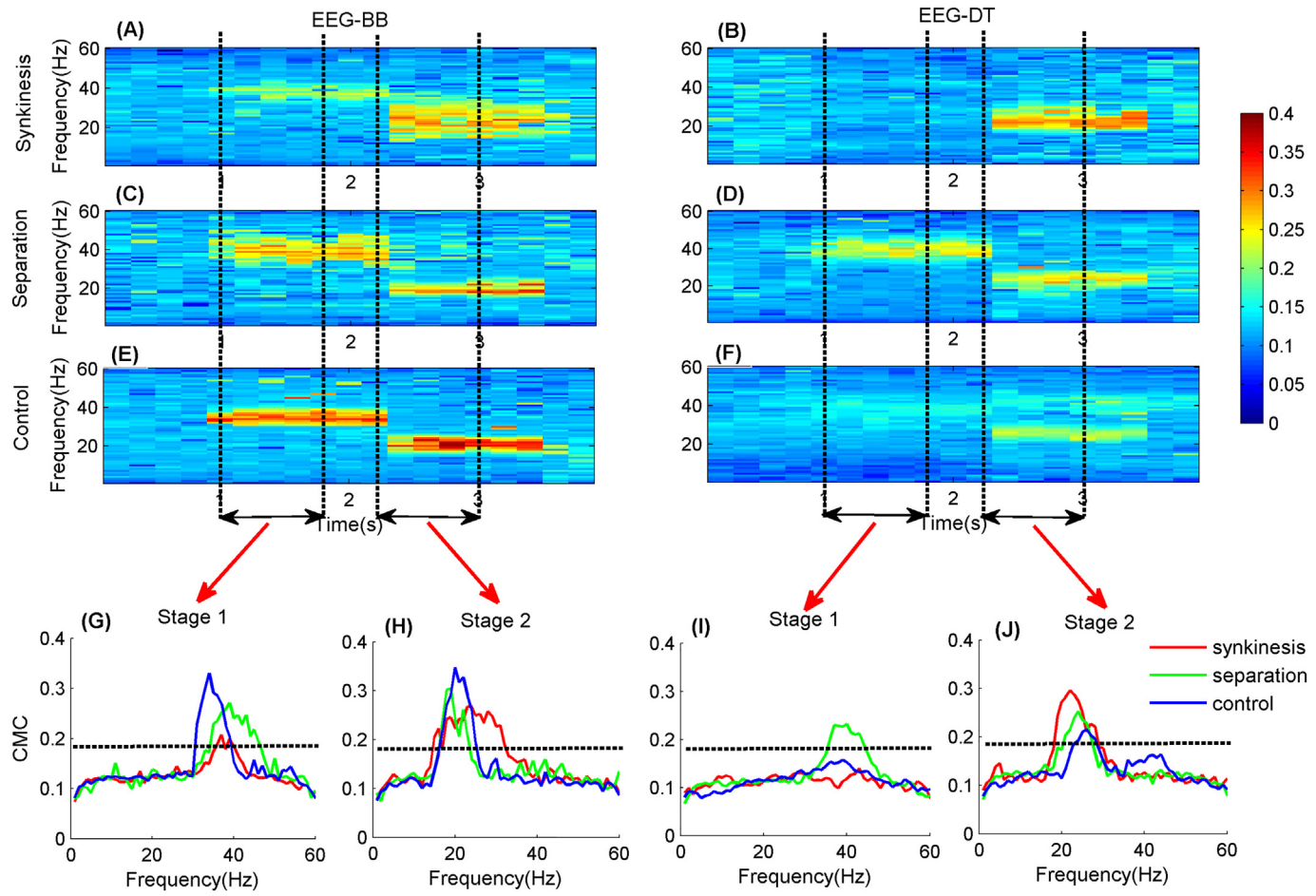


**Fig. 6.** Group-average corticomuscular coherence between EEG and EMG of BB and DT muscles, for each muscle, A and B shows its coherence with the scalp areas for the synkinetic patients, C and D for separate patients and E and F for controls. For A, B, C, D, E and F, the y-axis is frequency, the x-axis is time, and the color bar indicates the level of coherence (red, higher level; blue, lower level). G, H, I and J show the mean coherence values based on EEG and EMG signals from 2.5 to 4.5 s and from 5.5 to 7.5 s, corresponding roughly from the beginning to the end of reaching movement. (For interpretation of the references to color in this figure legend, the reader is referred to the web version of this article.)

coherence in EEG-DT combination. In contrast, for stroke patients, though reduced coherence was at gamma-band in EEG-BB for separate phase and absent coherence for synkinetic phase during stage 1 (Fig. 6(G)), high coherence in EEG-DT combination for separate phase (Fig. 6(I)). Similarly, though reduced coherence was at gamma-band in EEG-BB for synkinetic and separate phase during stage 2 (Fig. 6(H)), high coherence in EEG-DT combination for synkinetic and separate phases (Fig. 6(J)).

To investigate the differences between stroke patients and healthy controls in both stage 1 and stage 2, four-way rANOVA was performed with subject (3 levels: synkinesis, separation and control), stage (2 levels: stage 1 and stage 2), muscle (2 levels: EEG-BB and EEG-DT) and frequency band (2 levels: beta and gamma) as within-subject factors, and the $A_{coh}$ value as the dependent variable. Four-way rANOVA showed a main effect for subjects ($F(2,21) = 13.255$, $p = 0.000$), and pairwise comparison showed that stroke patients with synkinesis had lower corticomuscular interaction compared to patients with separation ($p = 0.000$, Bonferroni correction) and healthy controls ($p = 0.002$, Bonferroni correction). Additionally, there yielded significant main effects for muscle ($F(1,21) = 48.508$, $p = 0.000$) and frequency band ($F(1,21) = 8.926$, $p = 0.007$). Fig. 7 described the differences among synkinetic patients, separate patients and healthy controls in different conditions. Under stage 1, there was a significant difference among synkinetic patients, separate patients and healthy controls ($F(2,21) = 39.472$, $p = 0.000$). Pairwise comparison with multiple correction showed that stroke patients with synkinesis had lower corticomuscular interaction compared to patients with separation ($p = 0.000$, Bonferroni correction) and healthy controls ($p = 0.000$, Bonferroni correction). In EEG-BB combination, there were significant differences at beta ($F(2,21) = 13.15$, $p = 0.000$) and gamma ($F(2,21) = 25.83$, $p = 0.000$) bands among synkinetic patients, separate patients and healthy controls. Pairwise comparison with multiple correction showed that stroke patients had lower corticomuscular interaction at beta-band compared to healthy controls (synkinetic: $p = 0.001$, Bonferroni correction; separate: $p = 0.001$, Bonferroni correction), while in EEG-DT combination, separate stroke patients had lower corticomuscular interaction at gamma-band compared to synkinetic ones ($p = 0.000$, Bonferroni correction) and healthy controls ($p = 0.000$, Bonferroni correction). Under stage 2, although there was no significant difference among synkinetic patients, separate patients and healthy controls ($F(2,21) = 1.197$, $p = 0.322$), in EEG-BB combination, synkinetic patients had lower corticomuscular interaction at beta-band compared to separate patients ($p = 0.017$, Bonferroni correction) and healthy controls ($p = 0.000$, Bonferroni correction), and separate patients had lower corticomuscular interaction than healthy controls ($p = 0.004$, Bonferroni correction). In EEG-DT combination, synkinetic patients had higher corticomuscular interaction at beta-band compared to separate patients ($p = 0.000$, Bonferroni correction) and healthy controls ($p = 0.000$, Bonferroni correction).

### 3.4. Relation between FCMC and the relevant factors

In order to investigate the influence between the coherence and the motor performance, EMG or EEG power spectral and clinical assessment scale, the statistical analysis were carried out.

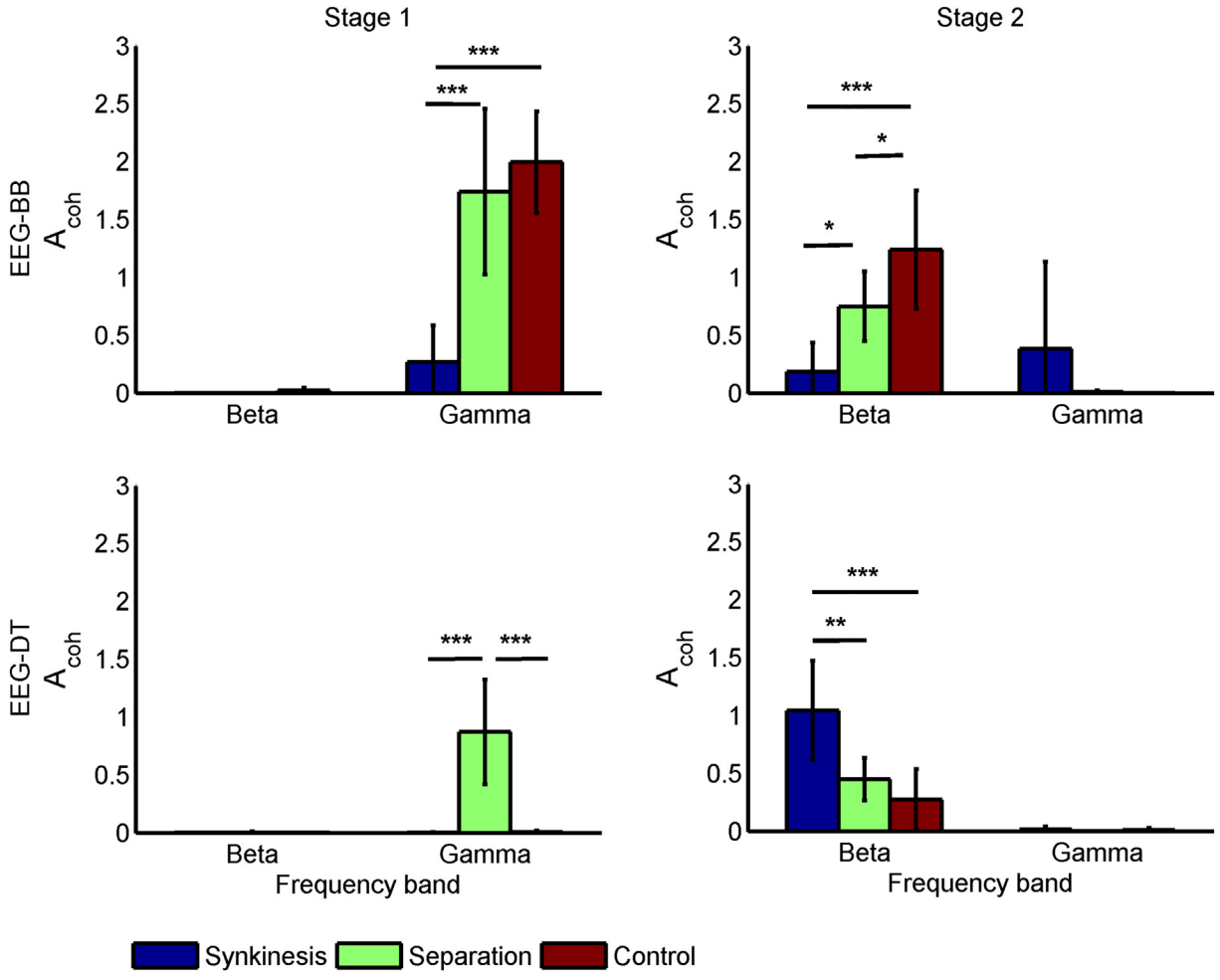


**Fig. 7.** Comparison of the $A_{coh}$ values among synkinesis, separation and control in different conditions.

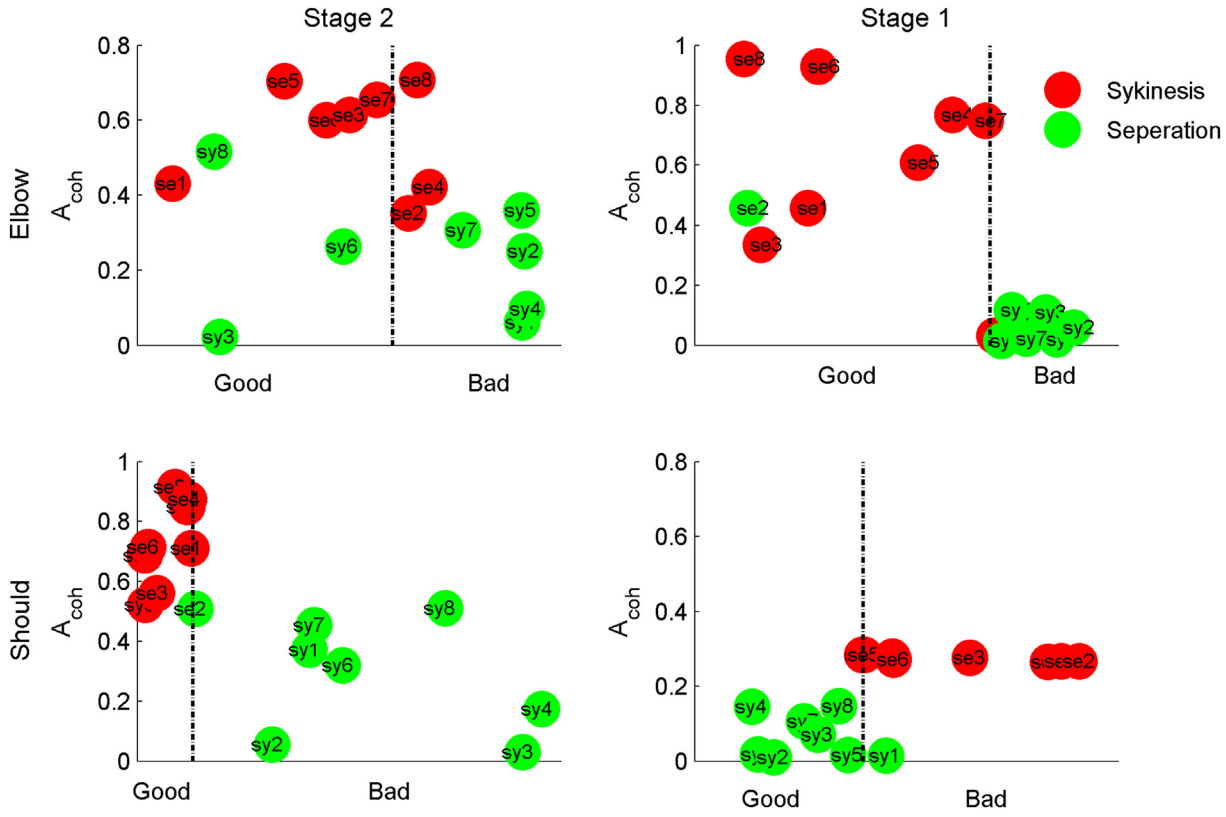


**Fig. 8.** Result between the $A_{coh}$ values and the motor performance under elbow and shoulder joints movement in both stage 1 and stage 2, respectively. The circles represented stroke patients, and the green denoted synkinetic patients and red for separate patients. The label inside the circle denoted the attribute of the participants, where 'se' was the patients with the separation phase and 'sy' was the patients with synkinetic phase.

*3.4.1. Relation between FCMC and motor performance*

In order to explore the correlation between the FCMC and the motor performance, we firstly divided $AA\_MSE_{mean}$ and $A\_MSE_{mean}$ values across all stroke patients into two groups, respectively, according to the detailed description in the Section 2.4. We then calculated the significant area $A_{coh}$ values according to the formula (8). Additionally, considering that the elbow and shoulder joints movement in the designed task mainly played a role in the calculation of EEG-BB and EEG-DT combinations, respectively, we analyzed the relationship between the $A_{coh}$ values in the EEG-BB combination and the angles values of elbow joint, and the relationship between the $A_{coh}$ values in the EEG-DT combination and the angles values of shoulder joint. After that, we plotted the $A_{coh}$ values on the basis of the error distribution from small to big errors. Fig. 8 showed the results between the $A_{coh}$ values and the motor performance under the elbow and shoulder joints movement in both stage 1 and stage 2, respectively. In this figure, the circle represented the stroke patients, and the green denoted the synkinesis and red for separation. The label inside the circle denoted the attribute of the participants, where 'se' was the stroke patients with separation, and 'sy' was the patients with synkinesis. As Fig. 8 was shown, there was a significant difference between the 'bad' and 'good' groups. Except for Fig. 8(D), Fig. 8(A), (B) and (C) showed that most stroke patients with separation movement performed 'good' motor performance, and most stroke patients with synkinesis performed 'bad' motor performance. These results were consistent with the results in the Sections 3.1 and 3.3. On the contrary, Fig. 8(D) showed that most stroke patients with separation performed 'bad' motor performance, and most stroke patients with synkinesis performed 'good' ones. In brief, the FCMC was related to the motor performance.

*3.4.2. Relation between FCMC and EMG/EEG power spectral*

To examine the possible association between the FCMC and the spectral power of EMG or EEG signals, we calculated the spectral power $A_{pow(f_l \sim f_h)}$ and the significant area $A_{coh}$ at each frequency band. Considering that significant coherence was mainly at both beta and gamma bands, we only took the beta and gamma bands into account. In this study, the possible associations were analyzed between the $A_{coh}$ values (stage 1 and stage 2) and the $A_{pow(f_l \sim f_h)}$ values for EMG under different cases (BB: beta and gamma bands; DT: beta and gamma bands), and between the $A_{coh}$ values (stage 1 and stage 2) and the $A_{pow(f_l \sim f_h)}$ values for EEG (the mean values of EEG signals over CP3, CP5, FC3, FC5, C3 and C5 channels) under different cases (beta and gamma bands). Tables 2 and 3 showed the analyzed results for EMG and EEG, respectively. However, no correlation was examined for both EEG and EMG power spectral.

*3.4.3. Relation between FCMC and clinical assessment scale*

To analyze the relationship between the FCMC and the clinical assessment scale for stroke patients, we performed person correlation analysis between the significant area $A_{coh}$ values and the STM test (see Fig. 1). Fig. 9 showed the results under stage 1 and stage 2 in both EEG-

**Table 2**
Correlation coefficient between the $A_{coh}$ values and the $A_{pow(f_l \sim f_h)}$ values of EMG signal at beta and gamma bands.

| Muscle | Frequency band | Correlation coefficient | |
|---|---|---|---|
| | | Stage 1 | Stage 2 |
| BB | Beta | 0.004 | 0.305 |
| | Gamma | 0.459 | 0.211 |
| DT | Beta | −0.079 | −0.137 |
| | Gamma | 0.412 | −0.301 |

*p < 0.05 (Pearson's correlation coefficients).
**p < 0.01 (Pearson's correlation coefficients).

**Table 3**
Correlation coefficient between the $A_{coh}$ values and the $A_{pow(f_l \sim f_h)}$ values of EEG signal at beta and gamma bands.

| Frequency band | Correlation coefficient | |
|---|---|---|
| | Stage 1 | Stage 2 |
| Beta | 0.245 | 0.187 |
| Gamma | 0.201 | −0.062 |

*p < 0.05 (Pearson's correlation coefficients).
**p < 0.01 (Pearson's correlation coefficients).

BB and EEG-DT combinations, respectively. As Fig. 9 was shown, there were strong positive correlations between the $A_{coh}$ values and the STM test for all cases (r > 0.7, p < 0.01).

## 4. Discussion

This study mainly focused on FCMC between the motor cortex and the muscle in stroke patients and explored the differences between the synkinetic and separate stroke patients. Compared to healthy controls, stroke patients had abnormally reduced coherence in EEG-BB combination and increased coherence in EEG-DT combination. All these results illustrated stroke patients had abnormal functional corticomuscular coupling in sensorimotor system. For stroke patients, plenty of motor neurons in DT muscle were activated to trigger large scale abduction with shoulder joint, which was inconsistent with the controls. Compared to synkinetic stroke patients, separate stroke patients exhibited significant higher coherence at gamma-band during stage 1 in both EEG-BB and EEG-DT combinations, and higher coherence at beta-band during stage 2 in EEG-BB combination, but lower coherence at beta-band during stage 2 in EEG-DT combination. Though synkinetic stroke patients exhibited larger scale of abduction with shoulder joint and larger scale of DT muscles than separate stroke patients, we found there was no correlation between the FCMC and the EMG power spectral. We infer that various neurophysiological differences, the differences between BB and DT muscles, and motor performance, could be the influence factors on the FCMC.

### 4.1. Distinction between synkinesis and separation following stroke

Stroke patients, after rehabilitation for several weeks, will step into a new stage—synkinetic movement (P et al., 2011). In this stage, patients often do action with many sets of joints and muscles, while little voluntary movement with single joint (Lan, 2017). Two specific motor patterns with many sets of joints often appeared in this stage: flexor pattern in upper limb and extensor pattern in lower limb (Brunnstrom, 1970; Twitchell, 1951). After the synkinetic phase, stroke patients will meet another phase named separation. Unlike to the synkinetic phase, stroke patients can carry out pieces of movements with independent joint and muscle. In this study, the designed movement was “uplift the affected hand to reach the ipsilateral ear”, which is a typical movement in STM test to identify the recovery phase between the synkinesis and separation for stroke patients. During the movement of uplifting the arm, controls made a standard action that the BB muscle contracted largely and the DT muscle contracted a little. As a result, the elbow angle was in a reasonable range and the EMG signal in BB muscle was large, while a little for elbow angle and EMG signal in DT muscle. However, for stroke patients, especially for stroke patients with synkinesis, large scale of shoulder abduction appeared accompanied with the elbow flexion. Though the elbow angle was in a reasonable range, the EMG signal in BB muscle was lower and that in DT muscle was larger than those for controls. All these indicated a strong coupling was between the elbow flexion and shoulder abduction (Sukal et al., 2007). Similar results are also found in the study of the coupling analysis between the shoulder and hand movements (Lan, 2017) and stroke patients need the abduction with shoulder joint to compensate the insufficient of flexion with elbow joint in upper limb movement.

In our study, the functional coupling for stroke patients was reduced compared to that for healthy controls in EEG-BB combination under both stage 1 and stage 2. The possible mechanism will be discussed in the next Sections 4.2 and 4.3. Additionally, we found that synkinetic patients had higher coupling than separate patients and healthy controls in EEG-DT combination under stage 2. Although the EMG power spectral in DT muscle was highest for synkinetic patients, there was no statistical correlation between the functional coupling and the EMG power spectral. This means that the increased coupling for synkinesis is not derived from the enhancement of the EMG power spectral. Previous study pointed out that the expression of flexion synergy resulted from increased shared neural drive to the shoulder abductor and wrist/finger flexors (Lan, 2017). Hence, we can infer that this abnormally increased coupling may spring from the “flexion synergy”. The overlap of shoulder and elbow joint representations at the cortical cortex leads to the coupling difference between the EEG-BB and EEG-DT combinations.

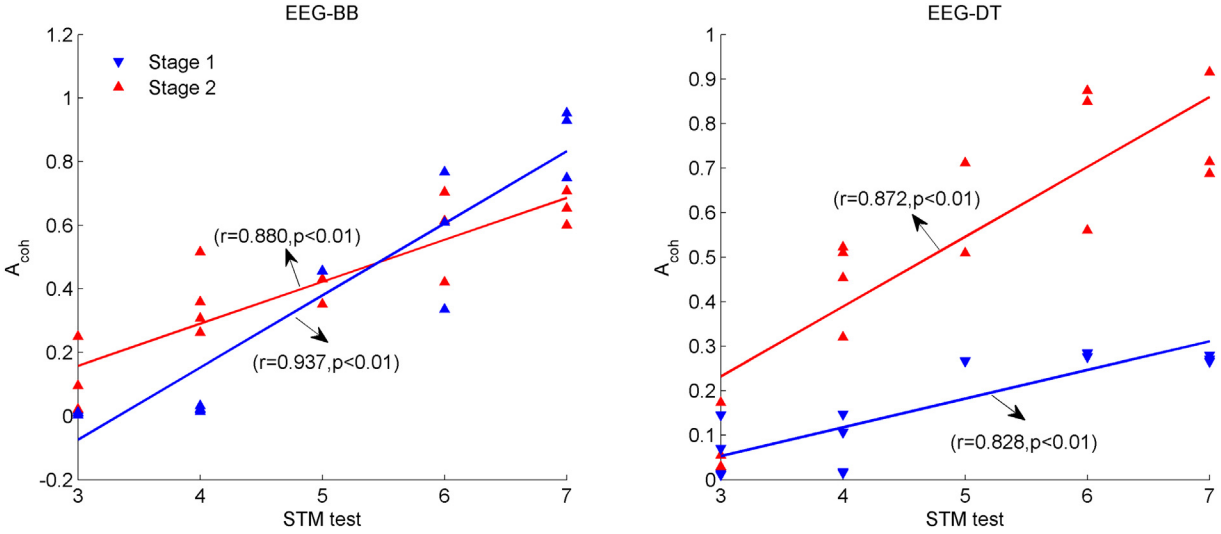


**Fig. 9.** The relationship between the FCMC and the STM test for stroke patients. We performed person correlation analysis between the significant area $A_{coh}$ values and the STM test under stage 1 and stage 2 in EEG-BB and EEG-DT combinations, respectively. There were strong positive correlations between the $A_{coh}$ values and the STM test for all cases (r > 0.7, p < 0.01).

When stroke subjects with synkinesis perform a steady-state task, partial function of the cortical cortex controlling on the elbow flexion may add on the shoulder abduction, which makes more efferent information act on the shoulder joint and DT muscle to execute the abduction movement. As a result, the coupling for synkinesis was higher than that for separation even control.

On the contrary, for separate stroke patients, the controls from the elbow representation may be decreased due to the relative independence between the shoulder and elbow joint, so the coupling was lower than that for synkinesis. However, separate stroke patients had higher coupling in the EEG-DT combination under stage 1. Similar to synkinetic stroke patients, separate stroke patients also showed that abnormal coupling in EEG-DT combination did not result from the EMG power spectral due to nothing between the FCMC and the EMG power spectral. Long-term poor movement, we also can infer, need for dynamic force output, though the separate stroke patients can control the elbow movement independently in a certain extent. For synkinetic stroke patients, the ability of integration information is weak to bring forth the gamma oscillation in EEG-DT combination although they get even poorer movement. To make a long story short, though stroke patients need integrate more information for shoulder abduction to compensate for the loss of elbow flexion, the compensatory mechanism may be difference. Stroke patients with synkinesis exhibited higher coupling at beta-band in EEG-DT combination due to partial elbow representation in cerebral cortex on the shoulder, while patients with separation showed higher coupling at gamma-band in EEG-DT combination due to the integration of more information in sensorimotor system.

### 4.2. Absent corticomuscular coupling at gamma-band in stroke patients

The task in the stage 1 was to slowly lift their hands up to the chest within 3 s according to the tip with speed at 15°/s, which was a process of dynamic force output. In previous literatures, gamma-band oscillations were verified to relate with dynamic force output (Andrykiewicz et al., 2007; Mehrkanoon et al., 2014; Muthukumaraswamy, 2011; Omlor et al., 2007), which promotes functional integration of neural information (Herrmann et al., 2004; Miltner et al., 1999). In our study, healthy controls exhibited significant coherence at gamma-band in EEG-BB combination during stage 1. However, for stroke patients, there was reduced even none gamma-range coherence in EEG-BB combination. This was consistent with Y. Fang's research (Fang et al., 2009) that lower corticomuscular coherence for stroke patients was at lower gamma-band compared to controls. Similar results were also revealed in deafferented patients (Patino et al., 2008) and Parkinson patients (Grosse et al., 2002).

These changes may derive from a host of reasons. Omlor et al. (2007) pointed out the higher attention modulates the dynamic force output. The similar conclusion was also found in Bauer et al. (2006) that spatial tactile attention increased the gamma-band activity. All these researches provide some evidences in the dynamic force output associated to cognitions. Additionally, several researches pointed out that the proprioceptive feedback is obligatory for the generation of gamma-range coupling during dynamic force output (Cheyne et al., 2008; Omlor et al., 2007; Tecchio et al., 2008). Cortical gamma coherence was absent for non-perceived stimuli applied to one hand (Meador et al., 2002). These researches suggest that gamma-band coupling plays an important role in the tasks linked to somatosensory. The stage 1 with dynamic forces output in our task is complex because it requires lifting the arm at a constant speed and maintaining the movement in space, using proprioception, audio-visual feedback and space perception. During dynamic force output, the sensorimotor system resonates at gamma-range to integrate the visual and proprioceptive information to produce the appropriate motor command (Omlor et al., 2007). However, For stroke patients, brain lesion, to a certain extent, has an influence on the motor function (Rathore et al., 2002), then prolonged immobility may evoke degeneration of cognitive function (de Haan et al., 2006), atrophy of sensorimotor cortex (Hoane et al., 1998). All these changes maybe result in the FCMC decrease or absence at gamma-band.

### 4.3. Decreased corticomuscular coupling at beta-band in stroke patients

Compared to stage 1, the task in the stage 2 was to maintain static state up to the chest for 3 s, which was a process of static force output. In stage 2, the FCMC was significant at beta-band in EEG-BB combination for heathy controls, which is accorded with the prior literatures that the beta oscillations of EEG travel between sensorimotor cortex and corresponding muscle (Baker et al., 1997; Conway et al., 1995; Groß et al., 2000; Halliday et al., 1998; Mehrkanoon et al., 2014; Salenius et al., 1997). These results have shown that beta-rhythm mainly roots in primary motor cortex (Muthukumaraswamy and Johnson, 2004) and the oscillations in beta-band are associated with controlling and maintaining steady-state force. Some researches pointed out that the efferent motor information is sufficient to generate beta-band coupling (Mendezbalbuena et al., 2012; Witte et al., 2007). The similar conclusion was identified by Gerloff et al. (2006) in the research on patients with early brain lesions.

Unlike to the results in healthy controls, stroke patients with synkinesis also had significant lower corticomuscular coherence at beta-band than stroke patients with separation and healthy controls in EEG-BB combinations, which is consistent with previous studies that reported significantly lower corticomuscular coupling for the affected hand (Fang et al., 2009; Mima et al., 2001; von Carlowitz-Ghori et al., 2014). Several factors may contribute to these results. Reduced neural activity after brain injury and weak cortical-spinal synaptic connections might influence corticomuscular coupling (Meng et al., 2009). However, other reports have pointed out that some patients with excellent recovery have higher coherence than healthy controls (Braun et al., 2007; Graziadio et al., 2012). In their opinion, the compensatory increase of FCMC possibly contributes to reinstate connectivity after stroke. These differences may reflect the damage to the interactive connection between the brain and the muscles in the sensory-motor systems due to structural lesioning of the cerebral cortex, which may disrupt coordination, feedback, and information transmission. Therefore, it is more likely that multifarious parameters could lead to the diverse results.

### 4.4. Mechanism of motor performance effect on FCMC

The present study explored the correlation between the FCMC and motor performance in different conditions. As Section 3.4.1 was shown, the FCMC is related to the motor performance, which is consistent with previous literatures (Chen et al., 2013). Of course, some researches on FCMC hold different views (Divekar, 2013; Yang et al., 2009). In addition, we found that most separate stroke patients with higher $A_{coh}$ values performed ‘good’ motor performance, and most synkinetic patients with lower $A_{coh}$ values performed ‘bad’ motor performance. In other words, our results showed that better performance was associated with higher corticomuscular coupling. This conclusion was also in line with several previous studies (Kristeva et al., 2007; Witte et al., 2007), while others presented the opposite conclusions that there was an inverse relationship between corticomuscular coupling and motor performance (Divekar, 2013; Yang et al., 2009). The similar result also occurred in our study. Example for shoulder joint under stage 1, separate stroke patients with higher $A_{coh}$ values performed ‘bad’ motor performance, while synkinetic stroke patients with lower $A_{coh}$ values performed ‘good’ one. This was quite the opposite. One obvious reason may be due to the nature of the performed task, dynamic or static. Although two opposite results were found in our study, we tend to the conclusion that better performance contributed to higher corticomuscular coupling.

In fact, multi-aspect factors may contribute to the above results. Most researchers consider that higher corticomuscular interaction comes from high attention demands towards the motor task (Jantzen et al., 2001; Kristeva-Feige et al., 2002; Murthy and Fetz, 1996). In our study, although we believe that the synkinetic patients performing the task must be assessed with more attentions, it is hard to pay high attentions on performing the task due to the brain lesion. In contrast, it is easier for separate stroke patients and less but high attentions could be put into this task. Additionally, perceived difficulty may be a possible factor directly related to corticomuscular coupling, which is found by Divekar and John (2013). In this study, the execution of the task mainly replies on the flexion of the elbow joint, and to a certain extent, it is in the scope of separation. It is more difficult to perform this task for synkinetic patients than separate ones. Therefore, we hypothesize that stroke patients, especially for synkinetic patients, may overburden to finish this movement within their power, and this could induce instability in motor performance as a compensatory measure. In additionally, for stroke patients with long-term dysfunction, the brain cortex need relearn to master the motor skill (Hardwick et al., 2017). Therefore, motor instability not only can increase the proliferation of cortical activation (Ruffino et al., 2017), but also may decrease the brain function of the efferent control to muscles. For separate stroke patients, long-term exercise makes them have the ability to finish the task with better performance. The cortical cortex is activated in specific area to control the movement of the muscles correspondingly. As a result, it shows us that synkinetic stroke patients have stronger corticomuscular coupling than that for separate ones.

## Acknowledgments

XC and PX were responsible for the design of the research. XC, YZ and YC were charge of collecting and analyzing the data. XC and YC were responsible for relevant literatures. PX, XC and LZ provided the physiological mechanism for this discussion. XC, PX and SC drafted and integrated the manuscript. All authors have read and approved the final manuscript.

## Sources of funding

This research was supported by National Nature Science Foundation of China (grant number 61673336) and Natural Science Foundation of Hebei, China (grant number F2015203372).

## Declaration of interest

None.

## References

Andrykiewicz, A., Patino, L., Naranjo, J.R., Witte, M., Heppreymond, M.C., Kristeva, R., 2007. Corticomuscular synchronization with small and large dynamic force output. BMC Neurosci. 8, 1–12.
Baker, S., Olivier, E., Lemon, R., 1997. Coherent oscillations in monkey motor cortex and hand muscle EMG show task-dependent modulation. J. Physiol. 501, 225–241.
Bauer, M., Oostenveld, R., Peeters, M., Fries, P., 2006. Tactile spatial attention enhances gamma-band activity in somatosensory cortex and reduces low-frequency activity in parieto-occipital areas. J. Neurosci. 26, 490.
Braun, C., Staudt, M., Schmitt, C., Preissl, H., Birbaumer, N., Gerloff, C., 2007. Crossed cortico-spinal motor control after capsular stroke. Eur. J. Neurosci. 25, 2935–2945.
Brown, P., Salenius, S., Rothwell, J.C., Hari, R., 1998. Cortical correlate of the Piper rhythm in humans. J. Neurophysiol. 80, 2911–2917.
Brunnstrom, S., 1970. Movement therapy in hemiplegia. Neurophysiological Approach 113–122.
Chen, S., Entakli, J., Bonnard, M., Berton, E., De Graaf, J.B., 2013. Functional corticospinal projections from human supplementary motor area revealed by corticomuscular coherence during precise grip force control. PLoS One 8, e60291.
Chen, X.L., Xie, P., Zhang, Y.Y., Liu, L.X., Du, Y.H., Chen, X.L., Xie, P., Zhang, Y.Y., Liu, L.X., Du, Y.H., 2017. Distinction of functional corticomuscular coupling in synkinetic and separate movement following stroke. Brain Stimul. 10, 435–436.
Cheyne, D., Bells, S., Ferrari, P., Gaetz, W., Bostan, A.C., 2008. Self-paced movements induce high-frequency gamma oscillations in primary motor cortex. NeuroImage 42, 332–342.
Conway, B., Halliday, D., Farmer, S., Shahani, U., Maas, P., Weir, A., Rosenberg, J., 1995. Synchronization between motor cortex and spinal motoneuronal pool during the performance of a maintained motor task in man. J. Physiol. 489, 917–924.
De Clercq, W., Vergult, A., Vanrumste, B., Van Paesschen, W., Van Huffel, S., 2006. Canonical correlation analysis applied to remove muscle artifacts from the electroencephalogram. IEEE Trans. Biomed. Eng. 53, 2583–2587.
de Haan, E.H., Nys, G.M., Van Zandvoort, M.J., 2006. Cognitive function following stroke and vascular cognitive impairment. Curr. Opin. Neurol. 19, 559–564.
Divekar, N.V., 2013. Investigation of the Interaction Between Corticomuscular Coherence, Motor Precision and Perceived Difficulty in Wrist Flexion and Extension.
Divekar, N.V., John, L.R., 2013. Neurophysiological, behavioural and perceptual differences between wrist flexion and extension related to sensorimotor monitoring as shown by corticomuscular coherence. Clin. Neurophysiol. 124, 136–147.
Dpt, M.D.E., Ms, B.G.H., Acosta, A.M., Beer, R.F., Dewald, J.P.A., 2005. Modifiability of abnormal isometric elbow and shoulder joint torque coupling after stroke. Muscle Nerve 32, 170–178.
Fang, Y., Daly, J.J., Sun, J., Hvorat, K., Fredrickson, E., Pundik, S., Sahgal, V., Yue, G.H., 2009. Functional corticomuscular connection during reaching is weakened following stroke. Clin. Neurophysiol. 120, 994–1002.
Gerloff, C., Braun, C., Staudt, M., Hegner, Y.L., Dichgans, J., Krägelohmann, I., 2006. Coherent corticomuscular oscillations originate from primary motor cortex: evidence from patients with early brain lesions. Hum. Brain Mapp. 27, 789–798.
Graziadio, S., Tomasevic, L., Assenza, G., Tecchio, F., Eyre, J., 2012. The myth of the 'unaffected' side after unilateral stroke: is reorganisation of the non-infarcted corticospinal system to re-establish balance the price for recovery? Exp. Neurol. 238, 168–175.
Grinsted, A., Moore, J.C., Jevrejeva, S., 2004. Application of the cross wavelet transform and wavelet coherence to geophysical time series. Nonlinear Process. Geophys. 11, 561–566.
Groß, J., Tass, P., Salenius, S., Hari, R., Freund, H.J., Schnitzler, A., 2000. Cortico-muscular synchronization during isometric muscle contraction in humans as revealed by magnetoencephalography. J. Physiol. 527, 623–631.
Groß, J., Timmermann, L., Kujala, J., Dirks, M., Schmitz, F., Salmelin, R., Schnitzler, A., 2002. The neural basis of intermittent motor control in humans. Proc. Natl. Acad. Sci. 99, 2299–2302.
Grosse, P., Cassidy, M.J., Brown, P., 2002. EEG-EMG, MEG-EMG and EMG-EMG frequency analysis: physiological principles and clinical applications. Clin. Neurophysiol. 113, 1523–1531.
Grosse, P., Guerrini, R., Parmeggiani, L., Bonanni, P., Pogosyan, A., Brown, P., 2003. Abnormal corticomuscular and intermuscular coupling in high-frequency rhythmic myoclonus. Brain 126, 326–342.
Halliday, D.M., Conway, B.A., Farmer, S.F., Rosenberg, J.R., 1998. Using electroencephalography to study functional coupling between cortical activity and electromyograms during voluntary contractions in humans. Neurosci. Lett. 241, 5–8.
Hardwick, R.M., Rajan, V.A., Bastian, A.J., Krakauer, J.W., Celnik, P.A., 2017. Motor learning in stroke: trained patients are not equal to untrained patients with less impairment. Neurorehabil. Neural Repair 31, 178.
Herrmann, C.S., Munk, M.H.J., Engel, K.A., 2004. Cognitive functions of gamma-band activity: memory match and utilization. Trends Cogn. Sci. 8, 347.
Hoane, M.R., Irish, S.L., Marks, B.B., Barth, T.M., 1998. Preoperative regimens of magnesium facilitate recovery of function and prevent subcortical atrophy following lesions of the rat sensorimotor cortex. Brain Res. Bull. 45, 45–51.
Jantzen, K., Fuchs, A., Mayville, J.M., Deecke, L., Kelso, J., 2001. Neuromagnetic activity in alpha and beta bands reflect learning-induced increases in coordinative stability. Clin. Neurophysiol. 112, 1685–1697.
Kristeva, R., Patino, L., Omlor, W., 2007. Beta-range cortical motor spectral power and corticomuscular coherence as a mechanism for effective corticospinal interaction during steady-state motor output. NeuroImage 36, 785–792.
Kristeva-Feige, R., Fritsch, C., Timmer, J., Lücking, C.-H., 2002. Effects of attention and precision of exerted force on beta range EEG-EMG synchronization during a maintained motor contraction task. Clin. Neurophysiol. 113, 124–131.
Lan, Y., 2017. Mechanisms Underlying the Flexion Synergy and Hand Dysfunction Following Stroke: Implications for Neuro-prosthetics. Northwestern University.
McClelland, V.M., Cvetkovic, Z., Mills, K.R., 2012. Rectification of the EMG is an unnecessary and inappropriate step in the calculation of corticomuscular coherence. J. Neurosci. Methods 205, 190–201.
Meador, K.J., Ray, P.G., Echauz, J.R., Loring, D.W., Vachtsevanos, G.J., 2002. Gamma coherence and conscious perception. Neurology 59, 847–854.
Mehrkanoon, S., Breakspear, M., Boonstra, T.W., 2014. The reorganization of corticomuscular coherence during a transition between sensorimotor states. NeuroImage 100, 692–702.
Mendezbalbuena, I., Huethe, F., Schultemönting, J., Leonhart, R., Manjarrez, E., Kristeva, R., 2012. Corticomuscular coherence reflects interindividual differences in the state of the corticomuscular network during low-level static and dynamic forces. Cereb. Cortex 22, 628–638.
Meng, F., Tong, K.-Y., Chan, S.-T., Wong, W.-W., Lui, K.-H., Tang, K.-W., Gao, X., Gao, S., 2009. Cerebral plasticity after subcortical stroke as revealed by cortico-muscular coherence. IEEE Trans. Neural Syst. Rehabil. Eng. 17, 234–243.
Miller, L.C., Dewald, J.P., 2012. Involuntary paretic wrist/finger flexion forces and EMG increase with shoulder abduction load in individuals with chronic stroke. Clin. Neurophysiol. 123, 1216–1225.
Miltner, W.H.R., Braun, C., Arnold, M., Witte, H., Taub, E., 1999. Coherence of gamma-band EEG activity as a basis for associative learning. Nature 397, 434–436.
Mima, T., Hallett, M., 1999. Corticomuscular coherence: a review. J. Clin. Neurophysiol. 16, 501.

Mima, T., Toma, K., Koshy, B., Hallett, M., 2001. Coherence between cortical and muscular activities after subcortical stroke. Stroke 32, 2597–2601.
Müller, G., 1970. Movement Therapy in Hemiplegia. Medical Dept., Harper & Row.
Murthy, V.N., Fetz, E.E., 1996. Oscillatory activity in sensorimotor cortex of awake monkeys: synchronization of local field potentials and relation to behavior. J. Neurophysiol. 76, 3949–3967.
Muthukumaraswamy, S.D., 2011. Temporal dynamics of primary motor cortex γ oscillation amplitude and piper corticomuscular coherence changes during motor control. In: Experimental Brain Research. Experimentelle Hirnforschung. Expérimentation cérébrale. 212. pp. 623–633.
Muthukumaraswamy, S.D., Johnson, B.W., 2004. Primary motor cortex activation during action observation revealed by wavelet analysis of the EEG. Clin. Neurophysiol. 115, 1760–1766.
Myers, L., Lowery, M., O'malley, M., Vaughan, C., Heneghan, C., Gibson, A.S.C., Harley, Y., Sreenivasan, R., 2003. Rectification and non-linear pre-processing of EMG signals for cortico-muscular analysis. J. Neurosci. Methods 124, 157–165.
Oldfield, R.C., 1971. The assessment and analysis of handedness: the Edinburgh inventory. Neuropsychologia 9, 97–113.
Omlor, W., Patino, L., Hepp-Reymond, M.-C., Kristeva, R., 2007. Gamma-range corticomuscular coherence during dynamic force output. NeuroImage 34, 1191–1198.
P, M., SF, S., E, F., M, A., G, Z., FB, P., F, A., A, B., GM, T., P, B., 2011. Effect of median-nerve electrical stimulation on BOLD activity in acute ischemic stroke patients. Clin. Neurophysiol. 122, 142–153.
Patino, L., Omlor, W., Chakarov, V., Hepp-Reymond, M.-C., Kristeva, R., 2008. Absence of gamma-range corticomuscular coherence during dynamic force in a deafferented patient. J. Neurophysiol. 99, 1906–1916.
Raethjen, J., Lindemann, M., Dümpelmann, M., Wenzelburger, R., Stolze, H., Pfister, G., Elger, C.E., Timmer, J., Deuschl, G., 2002. Corticomuscular coherence in the 6–15 Hz band: is the cortex involved in the generation of physiologic tremor? Exp. Brain Res. 142, 32–40.
Rathore, S.S., Hinn, A.R., Cooper, L.S., Tyroler, H.A., Rosamond, W.D., 2002. Characterization of incident stroke signs and symptoms: findings from the atherosclerosis risk in communities study. Stroke 33, 2718–2721.
Rosenberg, J.R., Amjad, A.M., Breeze, P., Brillinger, D.R., Halliday, D.M., 1989. The Fourier approach to the identification of functional coupling between neuronal spike trains. Prog. Biophys. Mol. Biol. 53, 1–31.
Rossiter, H.E., Eaves, C., Davis, E., Boudrias, M.-H., Park, C.-H., Farmer, S., Barnes, G., Litvak, V., Ward, N.S., 2013. Changes in the location of cortico-muscular coherence following stroke. NeuroImage 2, 50–55.
Ruffino, C., Papaxanthis, C., Lebon, F., 2017. Neural plasticity during motor learning with motor imagery practice: review and perspectives. Neuroscience 341, 61.
Salenius, S., Portin, K., Kajola, M., Salmelin, R., Hari, R., 1997. Cortical control of human motoneuron firing during isometric contraction. J. Neurophysiol. 77, 3401–3405.
Stoica, P., Nehorai, A., 1988. Performance analysis of an adaptive notch filter with constrained poles and zeros. IEEE Trans. Acoust. Speech Signal Process. 36, 911–919.
Sukal, T.M., Ellis, M.D., Dewald, J.P.A., 2007. Shoulder abduction-induced reductions in reaching work area following hemiparetic stroke: neuroscientific implications. In: Experimental Brain Research.experimentelle Hirnforschung.expérimentation Cérébrale. 183. pp. 215–223.
Tecchio, F., Zappasodi, F., Porcaro, C., Barbati, G., Assenza, G., Salustri, C., Rossini, P.M., 2008. High-gamma band activity of primary hand cortical areas: a sensorimotor feedback efficiency index. NeuroImage 40, 256.
Twitchell, T.E., 1951. The restoration of motor function following hemiplegia in man. Brain J. Neurol. 74, 443.
von Carlowitz-Ghori, K., Bayraktaroglu, Z., Hohlefeld, F.U., Losch, F., Curio, G., Nikulin, V.V., 2014. Corticomuscular coherence in acute and chronic stroke. Clin. Neurophysiol. 125, 1182–1191.
Williams, E.R., Baker, S.N., 2009. Renshaw cell recurrent inhibition improves physiological tremor by reducing corticomuscular coupling at 10 Hz. J. Neurosci. 29, 6616–6624.
Witte, M., Patino, L., Andrykiewicz, A., Hepp-Reymond, M.-C., Kristeva, R., 2007. Modulation of human corticomuscular beta-range coherence with low-level static forces. Eur. J. Neurosci. 26, 3564–3570.
Yang, Q., Fang, Y., Sun, C.-K., Siemionow, V., Ranganathan, V.K., Khoshknabi, D., Davis, M.P., Walsh, D., Sahgal, V., Yue, G.H., 2009. Weakening of functional corticomuscular coupling during muscle fatigue. Brain Res. 1250, 101–112.
Yao, B., Salenius, S., Yue, G.H., Brown, R.W., Liu, J.Z., 2007. Effects of surface EMG rectification on power and coherence analyses: an EEG and MEG study. J. Neurosci. Methods 159, 215–223.
Yao, J., Chen, A., Carmona, C., Dewald, J.P., 2009. Cortical overlap of joint representations contributes to the loss of independent joint control following stroke. NeuroImage 45, 490–499.